American Journal of Mechanical Engineering, 2013, Vol. 1, No. 7, 417-422
Available online at http://pubs.sciepub.com/ajme/1/7/53

DOI:10.12691/ajme-1-7-53

Experimental Verification of Thrust Model Blower

Tomáš Lipták*, Ľubica Miková, Michal Kelemen, Erik Prada

Department of Applied Mechanics and Mechatronics, Faculty of Mechanical Engineering, Technical University of Košice, Košice, Slovakia
*Corresponding author: tomas.liptak@tuke.sk

Received October 22, 2013; Revised November 06, 2013; Accepted November 25, 2013

Abstract This article leads about the issue experimental verification of the thrust model blowers. In the framework of article were used the results of the Diploma thesis, which deals with design of mobile robot based on hovercraft [1]. In the first part of the article is described the first method testing of the maximum thrust of blower via deformation of the spring and second part is analyzed the second method testing via wood beam in the shape letter L. The main aim this article is to compare thrust indicated by the manufacturer with thrust experimental verified.

Keywords: *blower, spring, wood beam, microcontroller, thrust*

Cite This Article: Tomáš Lipták, Ľubica Miková, Michal Kelemen, and Erik Prada, "Experimental Verification of Thrust Model Blower." *American Journal of Mechanical Engineering* 1, no. 7 (2013): 417-422. doi: 10.12691/ajme-1-7-53.

1. Introduction

In Diploma thesis were created designs of variant solutions of the chassis of hovercraft, also other parts of the construction. Using the method of pairwise comparison was selected the most suitable variant, which was in the next phase in detail elaborated using program SolidWorks2011. Optimal variant was simulated in SolidWorks2011 and on the basis of results obtained from the simulation were selected drives with appropriately dimensioned power, shown in Figure 1 [1,5].

Figure 1. Final model of the hovercraft in program SolidWorks2011 [1]

For lift and movement of hovercraft were selected blowers of type GWS 40B 6000KV, which have a built-in three-phase brushless motor with revolution KV=6000 (6000 revolutions per minute to 1V). The engine belongs between the inrunners, because the rotor spins inside. This brushless motor was preferred before DC motor and it's mainly due to the performance and service life. DC battery voltage is to be transformed into a three alternating voltage with phase displacement 120°, which will be fed into the blower. This transformation of the DC voltage to AC voltage allows us regulators of brushless engines. For our blowers were selected regulators Xcontroller XC22-L, we can see in Figure 2 [1].

Figure 2. Testing bench for blowers via deformation of spring [1]

2. Testing of the Maximum Thrust Via Deformation of the Spring

This procedure of testing consists of measurement deformation spring of constructed dynamometer, which deforms in dependence on size of the thrust blower and using relation is this deformation recalculated on the thrust.

The blower is stored in PVC coupling with a diameter 50 mm. This PVC coupling is anchored by two adducent tapes on thin-walled L profile. Profile with blower and dynamometer are anchored on laboratory stand with double clamps. Blower and dynamometer are connected each other by carbine, which is fixed to blower by three copper wires relabeling insulating tape, shown in Figure 3 [1].

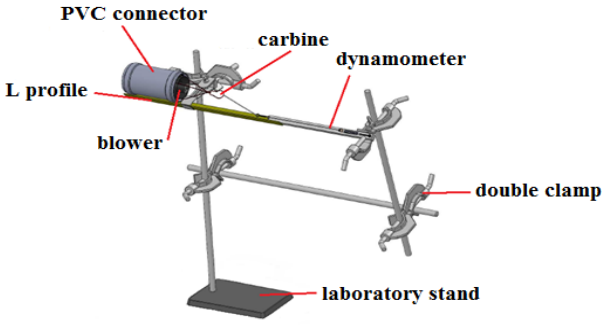

Figure 3. Testing bench for blowers via deformation of spring [1]

In the testing of the maximum thrust via deformation of the spring, microcontroller BasicATOM Pro 28-M is powered from laboratory source SP 150 and communicating with the PC needed for programming is secured using the RS232 interface, we can see in Figure 4. Resistive track of the potentiometer is powered from a 5V source SP 150 and regulator Xcontroller XC22-L is powered from laboratory source DIAMETRAL V130R50D. By moving the runner of potentiometer varies the size of the analog voltage to pine P0 of the microcomputer and from pin P4 is transmitted a modulated periodic signal with different impulse width, which is dependent on analog voltage. This dependence can be formulated by relation:

$$t_{imp} = \frac{2000}{65472}.U_{an} - 1000 \qquad (1)$$

where: t_{imp}[μs] – is impulse width

U_{an}[V] – analog voltage

This signal with different impulse width enters to regulator and causes a change revolution of the blower and subsequent deformation of the spring. During the measurement on oscilloscopes Voltcraft DSO-6250S was watched the changing pulse width from the microcomputer and the frequency of a one phase motor of the blower [1,2,3].

Program:

```
temp var word
a var sword
main
adin16 p0,temp
a=temp*2000/65472-1000
servo p4,a,10
goto main
```

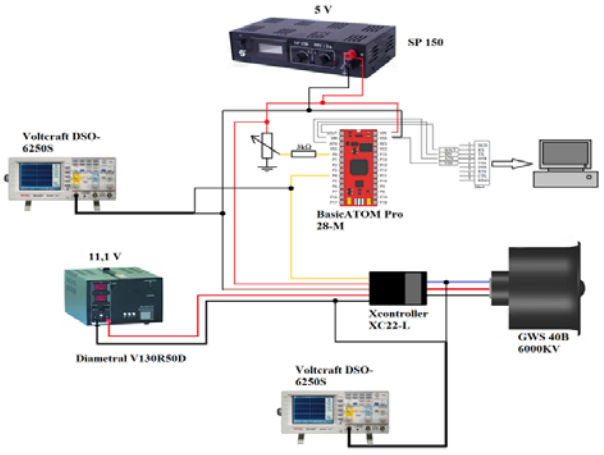

Figure 4. Scheme engagement with laboratory source DIAMETRAL V130R50D [1]

First, the maximum deflection of the spring was measured at the maximum of the pulse width, what we can see in Table 1. The biggest deformation caused the blower number 4, on which will be realized also further measurements [1].

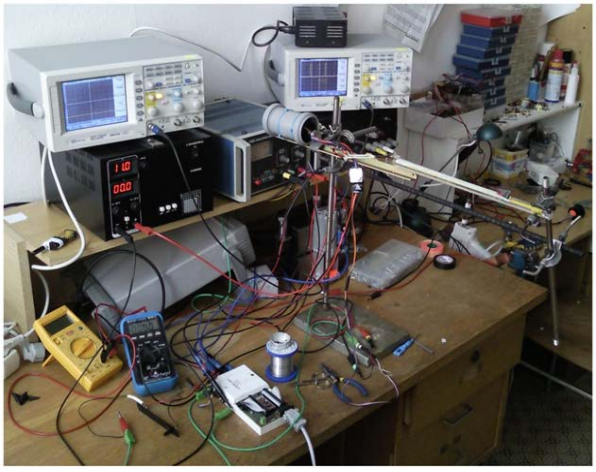

Figure 5. View to measuring progress [1]

Table 1. Maximum deformation of spring at the maximum impulse width [1]

blower	impulse BA [ms]	Δ [m]
no. 1	2	0,021
no. 2	2	0,021
no. 3	2	0,021
no. 4	2	0,0245

The measured values pulse width and frequency of one phase of the motor were read from Oscilloscopes and written into prepared table Table 2, from which was constructed graph, which we can see in Figure 6 [1].

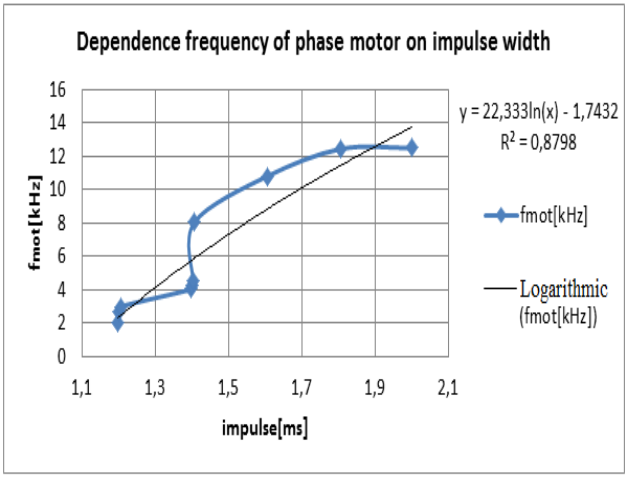

Figure 6. Graph dependence frequency of phase motor on impulse width [1]

On the previous graph we can see that the frequency phase of motor has logarithmic course with equation of reliability R^2=0,879. Uncertainty of the measured values created due to from problematic reading, because the values of the frequency and impulse width constantly varied.

Then on the laboratory source Diametral V130R50D were read the values of the entering current to the controller of blower at different frequencies and these values are written in Table 3 [1].

Table 2. Frequency motor for different impulse width [1]

blower n.4										
impulse BA [ms]	1,199	1,202	1,205	1,399	1,401	1,403	1,407	1,605	1,807	2,001
f_{mot} [kHz]	2,031	2,686	2,985	4,028	4,263	4,56	8,05	10,81	12,46	12,51

Table 3. Entering currents to regulator of blower for different frequencies [1]

blower n.4											
f_{mot} [kHz]	3,79	4,24	4,35	4,62	4,73	5,78	7,65	7,73	8,25	9,12	10,49
I [A]	0,6	1,1	1,6	1,9	2,2	2,9	4,0	4,8	5,4	6,8	7,7

From Table. 3 was constructed graph, shown in Figure 7, where the values of current obtained experimental varied according to the linear trend line with the equation of reliability R^2=0,977. Displacements of values also are created due to the variation in frequency [1].

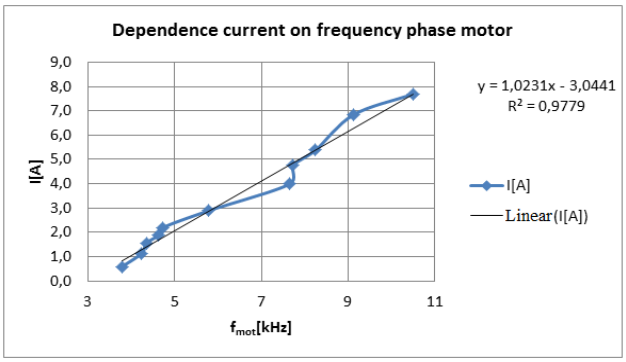

Figure 7. Graph dependence entering current to regulator on frequency phase motor [1]

On determination the thrust of blowers is necessary to determine the stiffness spring of dynamometer. By means of double clamp, dynamometer is clamped to a laboratory stand and on its end are gradually added weights. With the increasing weight is watched size deformation of spring and these values are recorded in Table 4 together with the calculated gravity force according to the relation [4,6]:

$$F_g = m.g \tag{2}$$

where: F_g[N] – is the gravity force acting on weights
m[kg] – the mass of weight
g[m.s^{-2}] – the gravity acceleration

Figure 8. View to measuring progress [1]

Table 4. Values needed to determine stiffness of spring [1]

m [kg]	0,05	0,08	0,1	0,12	0,13	0,15	0,17	0,18	0,2
F_g [N]	0,4905	0,7848	0,981	1,1772	1,2753	1,4715	1,6677	1,7658	1,962
Δ[m]	0,001	0,011	0,017	0,025	0,028	0,033	0,041	0,044	0,05

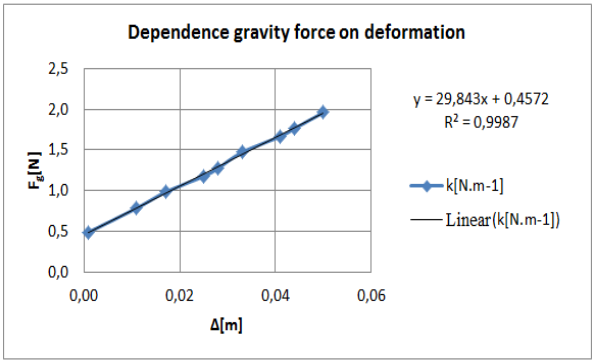

Figure 9. Graph dependence gravity force on deformation of spring [1]

From the graph, shown in Figure 9, after application of the linear trend line we get the prescription of function-stiffness of the springs with the equation of reliability R^2=0,9987.

From equilibrium of forces, shown in Figure 10, by neglecting friction between the contact surfaces of the blower and the inner cylindrical surface PVC coupling, we get the relation [7,8,9]:

$$F_d - F_k = 0. \tag{3}$$

After substituting the thrust force of blower:

$$F_d = m_t.g, \tag{4}$$

acting force on the spring:

$$F_k = k.\Delta, \tag{5}$$

and the stiffness into equation (3) and its adjustment we get the relation to calculate the thrust of blower:

$$m_t = \frac{k.\Delta}{g} = \frac{29,84.\Delta + 0,457}{g}, \tag{6}$$

where: m_t[g] – is the thrust of blower
k[N.m^{-1}] – the stiffness of spring
Δ[m] – the deformation of spring

Figure 10. Principled scheme engagement of blower with spring [1]

Values of deformation from Table 1 we will substitute into equation (6) and we will get thrust of blowers added into following table [1].

Table 5. Table of maximum deformation, which is added about thrust [1]

blower	impulse BA [ms]	Δ [m]	m_t [g]
no. 1	2	0,021	110,5
no. 2	2	0,021	110,5
no. 3	2	0,021	110,5
no. 4	2	0,0245	121,1

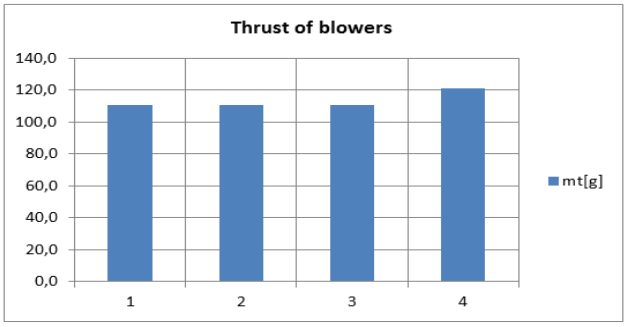

Figure 11. Column diagram of thrust blowers via the deformation of spring [1]

3. Testing of the Maximum Thrust Via Wood Beam in the Shape Letter L

The advantage of this method lies in the possibility of obtaining the values of the thrust blower directly without any calculations.

In this method of testing was used test bench consisting of wood beam in the shape of the letter L, which is stored in the bearings 6001 in wood supports, we can see in Figure 10. At the top of the beam is hole with a diameter 43 mm, which is created for mounting tested blower using insulation tape wrapped around a plastic cylindrical part of the blower, which prevents unwanted movement. At the bottom is the rubber foot attached using screw connection [1,2,3].

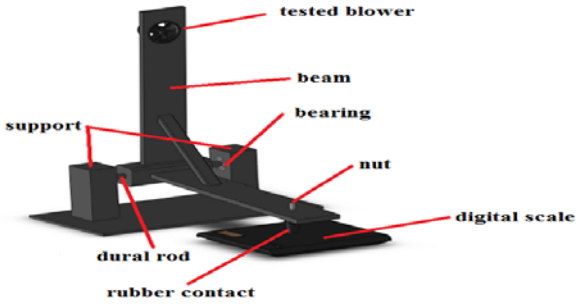

Figure 12. Test bench for blowers in SolidWorks2011 [1]

Distance between the axis of the hole for the blower and the joint must be the same as the distance between the joint and the axis of the rubber foot due to that thrust force of blower transfer through the rubber foot on digital weight SALTER 1066 in the ratio of 1: 1, shown in Figure 13. Calibration of digital weight has been confirmed by the manufacturer stated accuracy 1 g.

The scheme engagement and the program are the same as in the previous method of measurement. In this method of measurement is addition source Diametral in order to compare the values of the thrust also used Li-Polymer battery, we can see in Figure 14 [1].

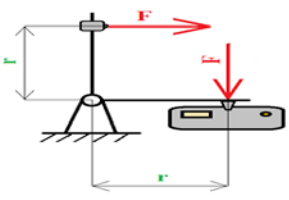

Figure 13. Principled scheme of test bench [1]

On blowers was measured their maximum thrust. They were powered from source Diametral V130R50D and also from Li-polymer battery, shown in Table 6. Thrust of blowers, which were powered from laboratory source, is lower, because the entering current to the blower at voltages 11V is until 16A and power supply has a current limit to 10A. For blower number 4 again was the biggest thrust [1].

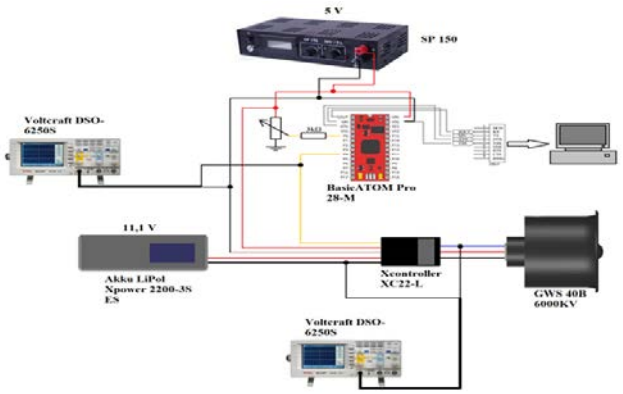

Figure 14. Scheme engagement with energy source Akku LiPol Xpower 2200-3S ES [1]

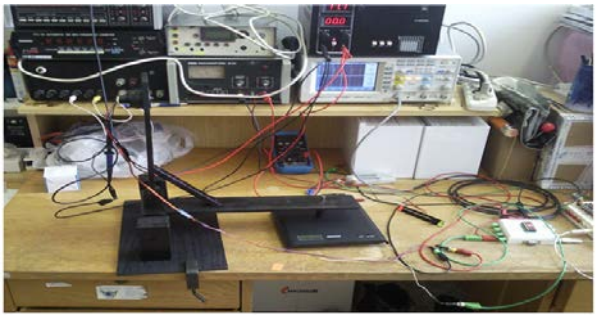

Figure 15. View to measuring progress [1]

Table 6. Tabuľka maximálnych ťahov [1]

blower		f_{mot} [kHz]			f_{aver} [kHz]	m_t [g]	impulse BA [ms]
no. 1	power supply	11,24	11,18	11,27	11,23	153	2
	battery	11,86	11,84	11,87	11,86	174	2
no. 2	power supply	11,25	11,26	11,21	11,24	163	2
	battery	9,4	9,39	9,36	9,38	202	2
no. 3	power supply	8,39	8,37	8,34	8,37	161	2
	battery	9,4	9,41	9,31	9,37	190	2
no. 4	power supply	11,53	11,55	11,49	11,52	164	2
	battery	9,45	9,42	9,41	9,43	208	2

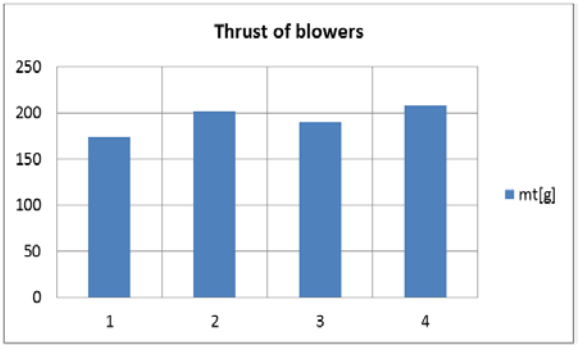

Figure 16. Column diagram of thrust blowers via the wood beam in the shape letter L [1]

Then was selected blower No.3 powered from laboratory source and was measured the frequency phase of motor and thrust at varying voltages, we can see in Table 7 [1].

Table 7. Table of frequencies and thrusts for different values of current [1]

blower no.3									
U [V]	f_{mot} [kHz]			f_{aver} [kHz]	m_t [g]			m_{taver} [g]	I[A]
6	-	-	-	-	-	-	-	-	-
7,4	6,16	6,23	6,15	6,18	98	96	97	97	6,6
8	6,79	6,81	6,74	6,78	111	110	110	110,33	7,4
8,5	7,26	7,14	7,16	7,19	124	126	126	125,33	8,1
9	7,63	7,65	7,64	7,64	140	141	139	140	8,8
9,5	8,05	8,03	8,02	8,03	152	153	154	153	9,5
10	8,36	8,37	8,41	8,38	165	164	163	164	10,1
10,5	8,36	8,33	8,34	8,34	163	162	163	162,67	10,1
11,1	8,39	8,37	8,34	8,37	164	165	163	164	10,1

In the previous table, we can see, that until at the voltage 7.4 V, the propeller of blower started to spin.

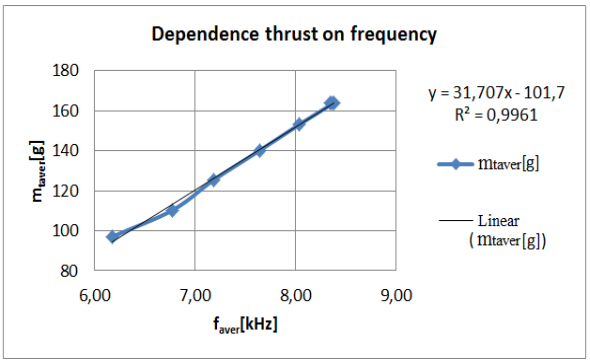

Figure 17. Graph of dependence thrust blowers on frequency phase motor [1]

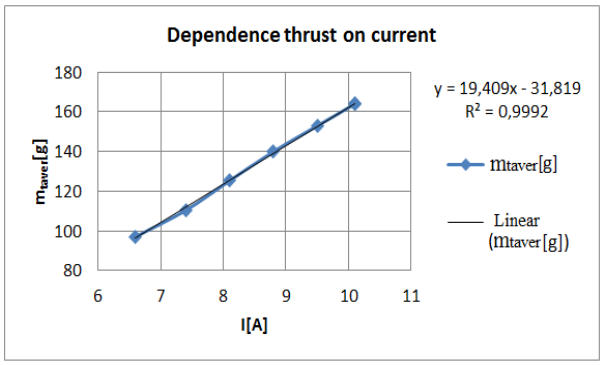

Figure 18. Graph of dependence thrust of blower on current [1]

The previous graphs show the dependences thrust of blower on frequency phase motor, electric current and voltage, which have linear course with the competent equations reliability R^2=0,996, R^2=0,999 and R^2=0,997. In Figure 19 we can see how at the voltage 10,5 V has not already increased thrust of blower, what is caused by current limit of laboratory source [1].

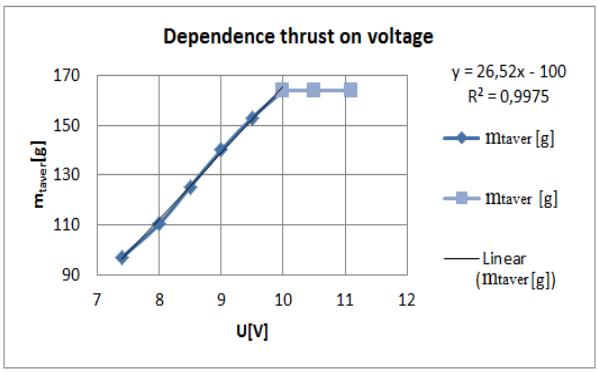

Figure 19. Graph of dependence thrust of blower on voltage [1]

4. Conclusion

In both cases testing of maximum thrust, we have obtained the values of thrust less than the value of thrust indicated by the manufacturer. The value of thrust indicated by the manufacturer at 11, 1V is 245g.

At the first method of testing, the values of thrust are smaller than at testing using L beam, what can be due to the fact that at moving the blower in a PVC coupling during measurement arises the friction between the contact surfaces. At testing with the using L beam are values of thrust larger, and it due to the fact that the beam together with clamped blower is stored in bearings, where arises less friction.

The blower number 2 and 4 due to higher thrust are used to lift and number 1 and 3 to move forward.

Acknowledgement

The authors would like to thank to Slovak Grant Agency – project VEGA 1/1205/12 “Numerical modeling of mechatronic systems”. This contribution is also result of the project VEGA MŠ SR for the support of this work under Project No. 1/0937/12. This contribution is also result of the project APVV-0091-11 “Using of methods of experimental and numerical modeling for increasing of competitiveness and innovation of mechanical and mechatronical systems”.

References

[1] Lipták, T., *Design of mobile robot based on hovercraft*, Diploma Thesis, Technical University of Košice, Košice, 2013.

[2] Liu Jitang, Li Zhouhang, Li Jianfeng and Flanagan, J.L, “Air Flow Simulation in High-pressure Air Blower with Splitter Blade,” *Electric Information and Control Engineering (ICEICE), 2011 International Conference on*, pp.1969-1972, 8-19 July. 2002.

[3] Jin-Woo Ahn, Huynh Khac Minh Khoi, Dong-Hee Lee, “Design and Analysis of High Speed 4/2 SRMs for an Air-Blower,” *Industrial Electronics (ISIE), 2010 IEEE International Symposium on*, pp. 1242-1246, 4-7 July. 2010.

[4] Jun-Young Lim, Yun-Chul Jung, Sang- Young Kim and Jung-Chul Kim, “High Efficiency and Low-Cost Switched Reluctance Motor for Air-conditioner Blower,” *Power Conversion Conference, 2002. PCC-Osaka 2002. Proceedings of the (Volume: 3)*, pp. 1460 - 1467, 02 Apr.2002-05 Apr.2002.

[5] Soe Myat Hein, Hwee Choo Liaw, “Design and Development of a Compact Hovercraft Vehicle,” in *2013 IEEE/ASME International Conference on Advanced Intelligent Mechatronics (AIM).*Wollongong. Australia, pp. 1516-1521.

[6] A. P. Aguiar, L. Cremean, J. P. Hespanha,“Position Tracking for io Nonlinear Underactuated Hovercraft: Controller Design and Experimental Results,” in *Proceedings of the 42nd IEEE*

Conference on Decision and Control. Maui, Hawaii USA, pp.3858-3863.

[7] Chun-Chieh, Wang, "Orientation Control of Hovercraft Systems via an SMFLC and Image-Guided Techniques," in *2011 IEEE International Conference on Fuzzy Systems.* Taipei, Taiwan, pp. 1138-1142.

[8] F. L. Roubieu, J. Serres, N. Franceschini, and S. Viollet, "A fully-autonomous hovercraft inspired by bees: wall following and speed control in straight and tapered corridors, "in *Proceedings of the 2012 IEEE, International Conference on Robotics and Biomimetics*. Guangzhou, China, pp. 1311-1318.

[9] R. Muñoz-Mansilla D. Chaos J. Aranda J.M. Díaz, "Application of quantitative feedback theory techniques for the control of a non-holonomic underactuated hovercraft, "in *IET Control Theory and Applications*. Madrid, Spain, pp. 2188-2197.